Study and design of antennas for WLAN MIMO applications

João Filipe Martins Ferreira
joaofmferreira@tecnico.ulisboa.pt

Av. Rovisco Pais 1, 1049-001 Lisboa, Portugal
Instituto Superior Técnico, Lisboa, Portugal

November 2016

Abstract

Recently, the use of wireless communications and especially WLAN networks has been growing. WLAN networks that use the IEEE 802.11n standard have a greater capacity for data transport as well as a higher communication speed. To achieve these requirements, MIMO systems present an adequate solution. Due to their reduced cost and straightforward manufacturing, printed antennas are in high demand for use in short range communications.

In this work, various printed double band MIMO antennas are presented, exploring spatial and polarization diversity, using the Rogers® rt/duroid 5880 substrate, fed by a coplanar waveguide, tuned to the frequencies of 2.45 and 5.6 GHz, from the Industrial, Scientific and Medical band (ISM). The structures were simulated in free space (S-parameter, radiation diagrams, correlation coefficient and diversity gain). Subsequently, the two element antenna that presented the best performance was chosen, and it was manufactured along with the four element antenna.

The performance of both antennas was analysed using the reflection and transmission coefficient measured in the laboratory. The obtained results were expected to be better in terms of the resonance of the antennas, however they were satisfactory in terms of the uncoupling. The manufactured antennas are suitable to use on WLAN in an indoor environment.

Keywords: WLAN; MIMO; Diversity;Dual-band; Rogers® rt/duroid 5880; Co-planar waveguide (CPW), Industrial, Scienfic and Medical band (ISM).

1. Introduction

Wireless comunications have been assumed a form of communication able to replace wire topology. All wireless local networks (WLANs) are based upon the IEEE 802.11 standard dor WLANs. With the improved performance offered by 802.11n, the standard soon became widespread with many products offered for its use. The idea behind this standard was that it would be able to provide a much better performance and to increase the link's speed. To achieve the desired fulfilment, a number of new features have been incorporated into IEEE standard to enable a higher quality. As such, in order to be able to carry very high data rates, 802.11n has utilised MIMO systems. The radio electric spectrum has become one of the most valuable goods for telecommunication operators and entities and MIMO technology ensures the maximum use of the available bandwidth. For each transmitter/receiver pair of antennas added to the system, the average capacity of a MIMO Rayleigh fading channel increases linearly (see figure 1 and [1]). Using different strategies such as spatial multiplexing, different types of diversity (time, frequency, space) and the required information coding, these goals can be achieved (as is shown in [2, 3]). In order to achieve these goals, to obtain an effective MIMO system, it is necessary to have enough uncorrelated antennas at the beginning and end of the link. In addition to the conventional antenna parameters, such as gain, radiation pattern and reflection coeficients, new parameters and aspects have to be considered in the design of MIMO systems, such as the mutual coupling and correlation between antennas. Facing these challenges, printed antenas are assumed to be the best choice for MIMO systems, due to its low-cost, easy fabrication and small dimensions.

2. State of the Art

2.1. Printed antennas

Electromagnetically printed antennas are developed to provide every wideband impedance characteristics. Many parameters optimize the impedance bandwidth of this antenna which has to be investigated. These antennas are built up for modern wideband wireless applications like mobile phones or Wireless LAN, Bluetooth, UWB and RFID tech-

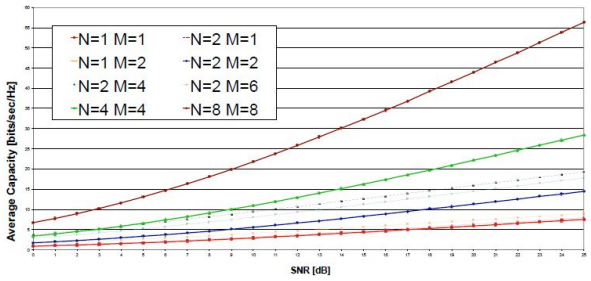

Figure 1: Average Capacity on a MIMO Rayleigh fading channel

nologies.

In [4, 5] two different antennas were designed in order to operate at 2.45 GHz frequency (ISM Band), on a FR4 substrate suitable for Body-Centric and wireless communications, fed by a Microstrip Line.

Circular Disc Monopole (CDM) with a a CPW feeding (using FR4 substrate, as well) with 50 Ohm impedance matched with the coaxial cable and two notches cut on the circular disk patch (used to increased the reflection coefficient at lower frequencies), as it shows [6], reveals to be an interesting solution for UWB applications.

A dual-band transparent antenna for ISM applications is studied in [7]. The antenna design consists of a circular radiating patch fed with a 50 Ohm CPW feeding and uses a transparent thin film material (AgHT-4) as substrate, with an overall size of $60 \times 60 \times 2.075mm^3$.

2.2. MIMO antenna solutions

In [8], several considerations concerning MIMO Antenna design are established in order to optimize aspects such as array configuration, radiation pattern, type of polarization and mutual coupling. This paper suggests different concepts and solutions for MIMO systems such as Antenna array configuration and reconfigurable antennas.

Antenna array or phased array system consist on a set of patch antennas with different layouts. The array topology is decided in order to maximize capacity and minimize error rate. In MIMO arrays, the correlation between the multiple signals must be as least as possible to counteract the scenario of degradation in channel capacity. Gain enhancement can be achieved by using several diversity strategies:

- Spatial Diversity: different elements are spaced with optimum distance to increase the number of channels in the link. In this technique, the smaller the distance, the more the mutual coupling between antennas, which result in a reduction of the channel capacity.
- Polarization Diversity: elements in the array are fed with differently polarized signals.
- Pattern Diversity: the signals with different angles are given to each one of the antennas present in the array.

An E-shaped triband printed monopole antenna suitable for WLAN applications is proposed in [9]. The dimension of the rectangular monopole is near $\lambda/4$, and two L-shaped patchs are added resulting in an E-shaped antenna, leading to a single frequency band antenna. According to the author an U-shaped current path is created with odd multiples of $\lambda/4$ length, introducing an extra resonant mode to be added to the initial E-shaped antenna structure. The third resonant mode was achieved by splitting the slot in two, adding an extra smaller U-shaped current path and resulting in a triband frequency response within the WLAN range. The presence of the slots does not influence the lower frequency, while the different slots and its width tunes the frequency of the second and third resonancy band.

MIMO arrays can be suitable for UWB applications, as it is reported on [10]. The author proposes a UWB MIMO antenna, with a bandwidth from 3.1 to 10.6 GHz, composed by two planar-monopole (PM) elements with 50 Ohm microstrip-fed placed perpendicularly to each other, in order to provide good isolation between the two input ports. For better matching at high frequencies, a small rectangular slot was cut on the upper edge of the ground plane. To increase isolation and impedance bandwidth, two long ground stubs were introduced, placed in parallel with the respective PM.

In [11] an antenna has been designed for 2.4/5.2/5.8 GHz WLAN and 2.5/3.5/5.5 GHz WiMAX applications that consists of two back-to-back monopole antennas, using a strategy to reduce the mutual coupling between two ports at the lower frequency band, introducing a T-shaped stub, where two rectangular slots are cut from the ground. A different approach is made in [12], where a compact microstrip patch antenna with four ports has been designed and implemented.

In [13] a directional shorted four-port patch antenna is introduced, fed with vertical probes which can operate either in dual linear and circular polarization modes in order to increase system capacity. The same concept is introduced on [14] structured with two printed F antennas on the top layer of a FR4 PCB with a rectangular ground plane underneath and a pair of quarter wavelength slot antennas inserted diagonally on the back side of the PCB.

3. Design and simulations

The design method started by choosing the materials used as well as the feeding technique. Then the operating frequencies and the patch shape were cho-

sen. Finally, the component's length was optimized in order to obtain the resonance at the intended frequencies, and there was also a readjustment of the antenna's overall size, to make it as small as possible. Firstly, a model of the simulated reference element will be presented as well as an explanation of the choices made in its construction. Then the simulated MIMO structures are presented. Initially, two element structures are shown utilising various types of diversity and showing various different configurations in order to choose the final structure to be manufactured. All the presented models simulated by CST Microwave Studio® software.

3.1. Reference Element

The basic element that was designed in order to build the proposed MIMO system is presented in figure 2. To obtain the corresponding designed dimensions, several parameters such as the slot's length and the spacing between the strip line and the ground plane had to be adjusted. In order to tune the frequencies for the required application and increase the resonance on these frequencies (2.45GHz and 5.8GHz), multiple parameter sweeps were made.

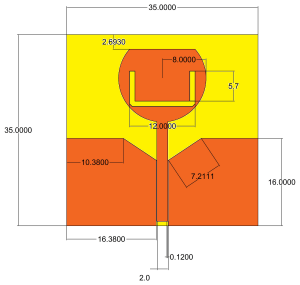

Figure 2: Dimensions of the reference element

The element is composed by a circular radiating patch with a U-slot that ensures resonance on the desired frequencies. A CPW feeding technique was used in order to reduce the circuit size and coupling and increase the design flexibility, as suggested on [15], [16],[17],[18]. Taking into account the available options at the DEEC prototyping room, the substrate chosen was Rogers® rt/duroid 5880.

To describe and analyse an antenna's behaviour as well as its operating band, the reflection coeficient is most commonly used. The absolute value of this parameter relates to antenna impedance matching and is defined by the ratio between the reflected power, P_r, to the antenna's incident power, P_i:

$$|S_{11}| = 10 \log_{10} \frac{P_r}{P_i} \tag{1}$$

To determine the operating band of an antenna there is one condition that must be satisfied:

$$\begin{cases} |S_{11}| \leq -10dB \\ P_r \leq P_i \times 0.1 \end{cases} \tag{2}$$

Observing figure 3, it can be concluded that the described element has two resonant frequency bands at 2.45 Ghz and 5.8 GHz (ISM operations), being described as a dual-band antenna.

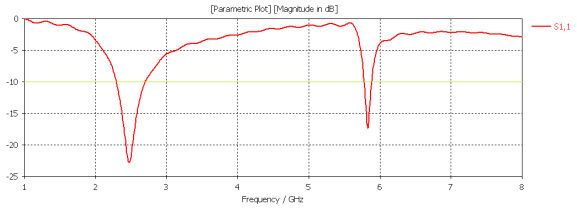

Figure 3: S-parameter for the reference element

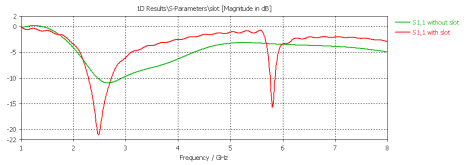

(a) S-parameter before and after introducing the U-slot

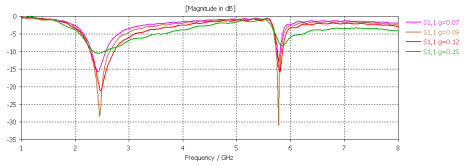

(b) Variation of S-parameter with spacing between the ground plane and the feeding line

Figure 4: S11 variation for the different parameters

In figure 4(a), it can be concluded that the U-slot presented on the patch ensures the resonance on the higher frequency (5.8GHz) and increases it on the lower frequency (2.45GHz) as well. In figure 4(b), the variation of the gap's length between the feeding line and the ground plane of the coplanar waveguide feed is shown. This parameter ensures resonance at the lower frequency and its value was initially chosen using the macros calculator available on the simulator. The optimum value was approximately 0.074 mm but due to limitations of the manufacturing process, the value chosen was 0.12 mm. Despite that, this value corresponds to the 50 Ohm impedance of the SMA Connector (figure 5).

In figure 6, a polar representation of the radiation pattern of the element of reference at 2.45 is shown.

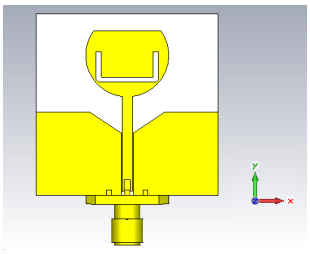

Figure 5: Geometry of the basic element with SMA connector.

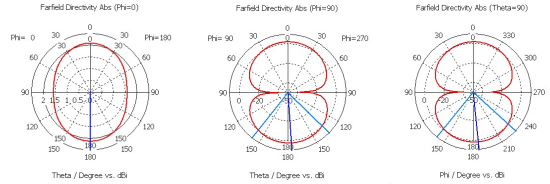

(a) $\Phi = 0^o$ (b) $\Phi = 90^o$ (c) $\theta = 90^o$

Figure 6: Radiation pattern for 2.45GHz of the element of reference in different planes

3.2. Two-element antennas

Significant SNR improvement and added gain is expected when using diversity systems, which are evaluated by three main parameters: correlation coefficient, diversity gain and antenna efficiency. On this paper, only correlation coefficient will be presented and discussed.

$$\rho_e = \frac{|S_{11}S_{12} + S_{21}S_{22}|^2}{((1 - (|S_{11}^2 + |S_{21}^2))(1 - (|S_{22}|^2 + |S_{12}^2)))} \quad (3)$$

All presented configurations are a basic addition of two referenced elements spaced by a substrate layer of 10mm (approximately $\lambda/12$ of the lowest frequency band). It is important to note that, in every 2-element antenna that will be proposed in this section, "port 1" refers to the element displayed on the left and "port 2" the other one.

Figure 7(a) refers to a structure that is composed by two reference elements displayed parallel to each other (spacial diversity).

Observing the S-parameter present in figures 7(b), it is noted that some mutual coupling between ports 1 and 2 is present, specially of the resonant frequencies (it's concluded because curves S_{11} and S_{22} overlap on S_{12} and S_{21}). However, the resonance at the higher frequency has registered a shift for lower frequencies (approximately 5.6GHz), which can be possible due to the mutual coupling registered. The correlation coefficient between ports shows satisfactory results, despite showing a peak very close to 5.3GHz.

Figure 8 illustrates a two-element MIMO antenna

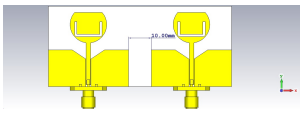

(a) Geometry

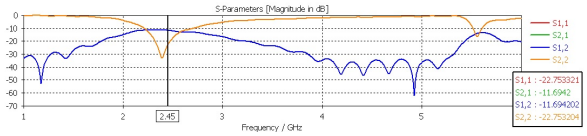

(b) S-parameter (mark at 2.45 GHz)

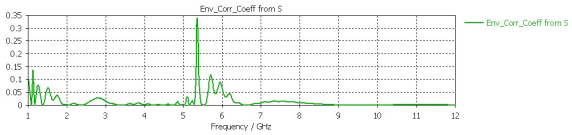

(c) Ports Correlation Coefficient

Figure 7: Geometry, S-parameter and port correlation coefficient of the structure designed with spacial diversity

using polarization diversity. The element on the left is placed horizontally, while the other is placed vertically, according to the perspective presented in figure 8(a) (the elements are placed orthogonally, resulting in polarization diversity). Comparing the results obtained with the structure previously investigated, it is concluded that mutual coupling has decreased, as well as the peaks of the correlation coefficient (approximately 0.08, figure 8(c)). However, the resonance at the higher frequency is at 5.6GHz, which still does not fulfill the requirements for a WLAN antenna (2.45 and 5.8GHz).

Figure 9 shows a similar structure presented in 8, but this time with inverted elements: the element on the left vertically and the other displayed horizontally. Thus, the elements are orthogonally disposed and polarization diversity is applied.

Observing figures 9(b) it is concluded that the results are good: both resonances are at the desired frequencies (the value at 2.45 and 5.8GHz for S_{11} and S_{22} are -27 and -22dB and -16 and -14dB, respectively). It is also noticed that the signals are completely uncoupled, which results in a good port correlation coefficient (the worst value is 0.027).

Figure 10 exhibits the same geometry shown on 9(a) in a larger scale in order to increase the space between the elements and therefore increase the isolation between them. The results regarding the S-parameter are good as is shown in figure 10(b). Correlation coefficient plot also shows reasonable values. Looking at the S-parameter results, signals appear to be perfectly decoupled. However, overall results are not better than those presented in figure 9. Furthermore, this geometry represents a higher overall size, which is an important factor in order

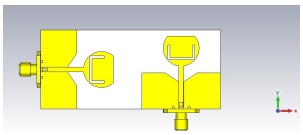

(a) Geometry

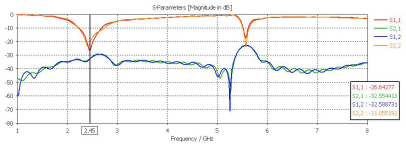

(b) S-parameter (mark at 2.45 GHz)

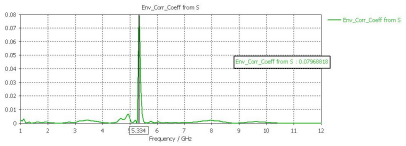

(c) Ports Correlation Coefficient

Figure 8: Geometry, S-parameter and Port correlation coefficients of a structure designed with polarization diversity

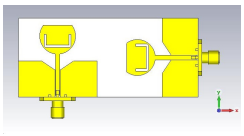

(a) Geometry

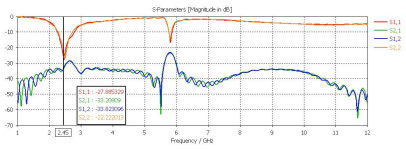

(b) S-parameter (mark at 2.45 GHz)

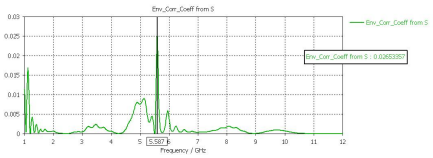

(c) Ports Correlation coefficient

Figure 9: Geometry, S-parameter and port correlation coefficients of a structure designed with polarization diversity, the element on the left is oriented according to the Y axis, while the other on X axis

to choose the best structure for WLAN applications (specially for mobile applications).

Analysing the discussed structures, the one that turns out to be the best solution for WLAN applications is the antenna simulated and presented in figure 9.

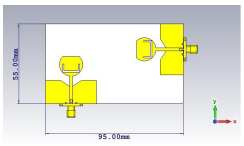

(a) Geometry

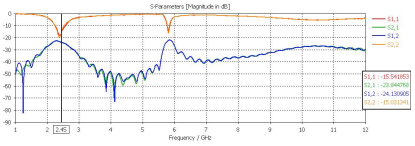

(b) S-parameter (mark at 2.45 GHz)

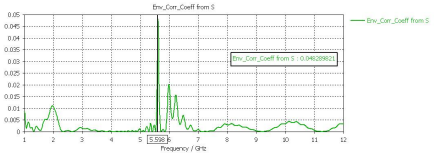

(c) Ports Correlation coefficient

Figure 10: Geometry, S-parameter and port correlation coefficients of a structure designed with polarization diversity, similar to the figure 9(a). The elements are spaced with 20mm.

3.3. Four-element antenna

As mentioned previously, by increasing the number of antennas presented on a MIMO system, the average capacity of the system increases almost linearly. Thus, adding this proposal to the goal of achieving an omnidirectional radiation pattern (that was not obtained with the two-element antennas designed), a structure was also studied and simulated with four elements, with a layout as shown in figure 11.

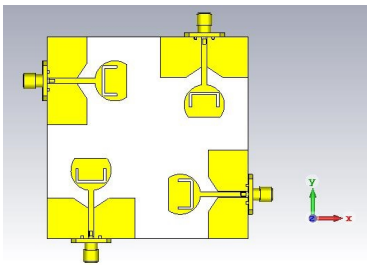

Figure 11: Configuration of the 4-element simulated and studied MIMO antenna.

As noted, the structure has four orthogonally arranged elements which ensure diversity polarization. Bearing in mind the above structures, this system has an area of 80x80mm^2. Each element is spaced 10mm towards its adjacent. Then the performance level of the S-parameter will be presented, as well as the correlation coefficient and diversity gain between each port. From here onwards, any references to the "port 1" corresponds to the port/element that is in the lower left corner. The

remaining ports are designated according to anticlockwise direction, i.e., "port 2" is the port of the lower right hand corner, "port 3" is in the upper right hand corner, and finally, "port 4" is associated with the upper left hand corner.

Note the symmetry of the proposed structure. It is concluded that, with respect to the S-parameter, there are only three curves to be taken into account: the reflection coefficient and the transmission coefficient between adjacent ports and between remote ports, which are arranged obliquely.

For a more neat analysis of the plot in the image 12 only the curves that are associated with port 1 are presented. As can be seen, there is a slight coupling at the frequency of 2.45GHz. However, in both the lowest and the highest resonant frequency, it is possible to verify that the desired -10dB are achieved.

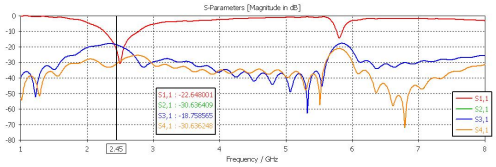

(a) S-parameter regarding to port1 (mark at 2.45GHz)

Figure 12: S-parameter (reflection and transmission coefficients) of the 4-element proposed Antenna

Due to the symmetrical structure of the presented antenna, only the results for port 1 were displayed (reflection coefficient and diversity gain).

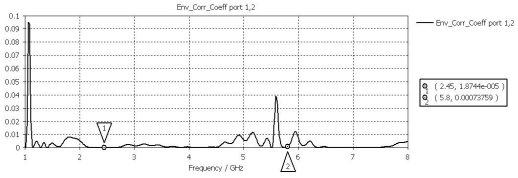

(a) Correlation coefficient between adjacent ports

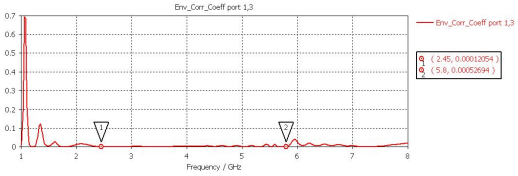

(b) Correlation coefficient between oblique ports

Figure 13: Correlation coefficient for the proposed antenna

Figure 13 shows the correlation coefficient between adjacent (subfigure 13(a)) and oblique (subfigure 13(b)) ports. It is observed that there is less isolation between oblique ports. However, in both cases, the great majority of the results are very reasonable.

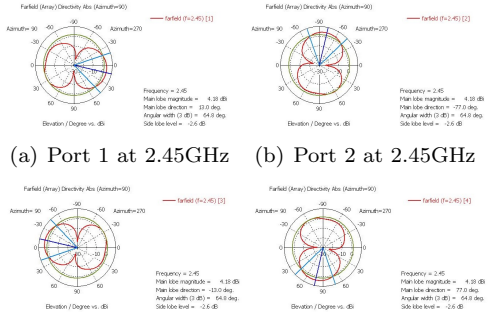

(a) Port 1 at 2.45GHz (b) Port 2 at 2.45GHz

(c) Port 3 at 2.45GHz (d) Port 4 at 2.45GHz

Figure 14: Radiation Diagram for 4-element antenna, polar representation at 2.45 and 5.8GHz

Figures 14 presents the radiation patterns polar form. In the figure, it is possible to observe that the initial goal considered while projecting a 4-element MIMO structure MIMO radiating in every direction reaching all the sectors (achieving an omnidirectional radiation pattern) was obtained. The angular width at -3dB for the frequency of 2.45GHz is of about 65°.

4. Prototype and experimental results

The results of the performance of the prototypes at the level of the S-parameter are presented (the two and four-element MIMO antennas). For the measurement of the parameters, the vector analyzer E8361A (VNA) from Agilent Technologies was used. A 1-9GHz band was defined with 1601 points, which results on a 5MHz step across the measured band. Coaxial cables of 1.2m were used.

4.1. Two-element MIMO antenna

As mentioned before, the proposed antenna that showed the best performance has been chosen to be manufactured is illustrated in figure 9. However, a failure of communication, led to an error that resulted in the antenna print shown in figure 8 instead of the initially desired one, as presented in figure 15.

Figure 15: 2-element antenna manufactured

The measured values for both resonant frequencies were well below expectations as it is observable

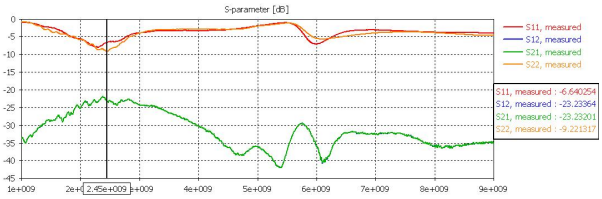

Figure 16: S-parameter measured at 2.45GHz

in Figure 16. The resonance at these frequencies is considerably smaller, which can be explained either by calibration errors, and also in the manufacturing process: the introduction of the SMA connector and the welding of the prototype. Another factor that may be relevant is the value of the spacing between the feed line and cpw, since, the ideal spacing of the reference element was not feasible in the laboratory where the antenna was fabricated.

Alternatively, the increase in the resonant frequency registered in the antenna measurements can also be explained by the possibility of some of the manufactured antenna dimensions to be slightly lower than the previously simulated model in CST.

However, it is noted that the resonant frequencies are visible, despite being small and diverting from the desired values and the simulation itself. Another positive point is that the signals are completely uncoupled, which is one of the main goals when creating a project of a MIMO antenna.

4.2. Four-element MIMO antenna

Figure 17 shows the manufactured structure corresponding to the simulated model (fig 11).

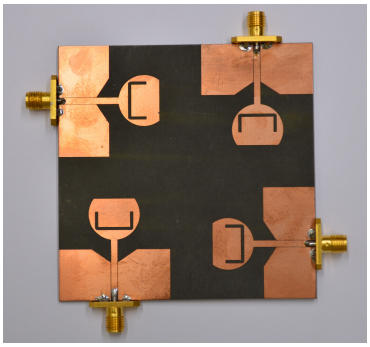

Figure 17: 4-element antenna maufactured

Figures 18 and 19 shows the results obtained experimentally. As was the case for the two antenna elements, it is observable that the recorded resonance for the desired frequency does not reach the threshold of -10dB, as was intended. However, especially for lower frequency (2.45GHz) the measured value is close to -8dB (5.8dB for the value is about -5dB). Yet, contrary to what was found earlier, the resonances are centered on the desired frequency.

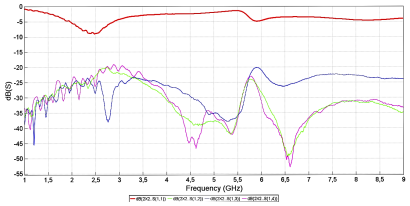

(a) S_{11} and S_{1j}

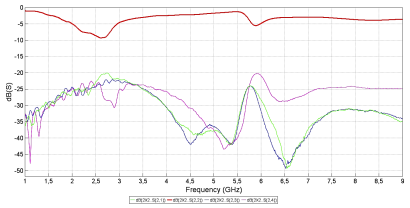

(b) S_{22} and S_{2j}

Figure 18: S-parameters measured (ports 1 and 2)

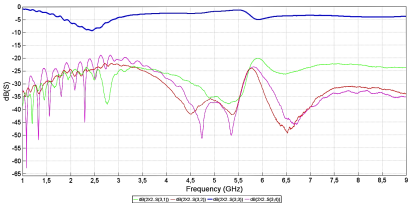

(a) S_{33} and S_{3j}

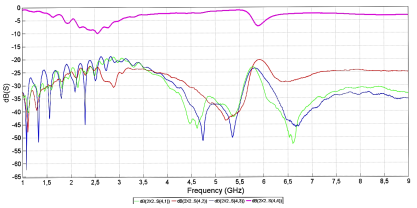

(b) S_{44} and S_{4j}

Figure 19: S-parameters measured (ports 3 and 4)

Again, in all the situations illustrated above, the signals are completely uncoupled, so one of the main objectives of the MIMO antenna was achieved.

According to the experimental results obtained, the prototype can be used as a wireless router apropriated for indoor environments, according to the IEEE 802.11n standard.

5. Conclusions

The work presented here has, as main objectives, the study and design of dual-band MIMO antennas, to operate in the ISM band of 2.45 5.8 GHz. The design of the structure was made using the CST Microwave Studio software, where were also carried out all the simulations of this work. A prototype was built and measured in the RF laboratory of the Institute of Telecommunications, Lisbon. A com-

munication failure resulted in printing an antenna mirroring the face of the mask and hence the construction of a structure symmetrical to the desired one (two elements). The results were not according to the expected, in terms of the value of the desired resonant frequency never reaching the -10dB barrier that was initially desired. However, it is noted that in both structures, a decoupling completion of the reflection coefficients and transmission was observed. One possible application for the built antenna is a wireless router indicated for indoor environments.

Possible future work is listed below:

- Improvement of the reference element to increase the resonance in the desired frequency;
- Taking measurements in order to obtain the efficiency of structures and their radiation patterns;
- Measurements of the manufactured structures in the presence of other electronic circuits inside of a plastic box).

References

[1] E. Mohamed and A. Abdulsattar, "Evaluation of mimo system capacity over rayleigh fading channel."

[2] S. Kumagai, R. Matsukawa, T. Obara, T. Yamamoto, and F. Adachi, "Spectral efficiency of distributed antenna network using mimo spatial multiplexing," in *Vehicular Technology Conference (VTC Fall), 2012 IEEE.* IEEE, 2012, pp. 1–5.

[3] X. Zhu and R. D. Murch, "Performance analysis of maximum likelihood detection in a mimo antenna system," *IEEE Transactions on Communications*, vol. 50, no. 2, pp. 187–191, 2002.

[4] B. Yeboah-Akowuah, P. Kosmas, and Y. Chen, "A low profile microstrip patch antenna for body-centric communications at 2.45 ghz band," in *2015 9th European Conference on Antennas and Propagation (EuCAP).* IEEE, 2015, pp. 1–3.

[5] P. N. Bhagat and V. Baru, "Slotted patch antennas with ebg structure for ism band," in *Communication, Information & Computing Technology (ICCICT), 2012 International Conference on.* IEEE, 2012, pp. 1–5.

[6] G. Tatsis, V. Raptis, and P. Kostarakis, "Design and measurements of ultra-wideband antenna," *International Journal of Communications, Network and System Sciences*, vol. 3, no. 02, p. 116, 2010.

[7] M. S. A. Rani, S. K. A. Rahim, A. Tharek, T. Peter, and S. W. Cheung, "Dual-band transparent antenna for ism band applications," *PIERS Proceedings, T aipei*, 2013.

[8] J. K. Babu, S. R. K. Krishna, and P. L. Reddy, "A review on the design of mimo antennas for upcoming 4g communications," *International Journal of Applied Engineering Research*, vol. 2, no. 1, p. 85, 2011.

[9] S. M. A. Nezhad and H. R. Hassani, "A novel triband e-shaped printed monopole antenna for mimo application," *IEEE antennas and wireless propagation letters*, vol. 9, pp. 576–579, 2010.

[10] L. Liu, S. Cheung, and T. Yuk, "Compact mimo antenna for portable devices in uwb applications," *IEEE Transactions on Antennas and Propagation*, vol. 61, no. 8, pp. 4257–4264, 2013.

[11] L. Xiong and P. Gao, "Compact dual-band printed diversity antenna for wimax/wlan applications," *Progress In Electromagnetics Research C*, vol. 32, pp. 151–165, 2012.

[12] Y. M. H. Sarah Hassan Khalaf, "Compact multiband mimo antenna for future wireless applications," *International Journal of Electrical and Electronics Research*, vol. 3, pp. 53–58, jan 2015.

[13] K. M. Mak, H. W. Lai, K. M. Luk, and C. H. Chan, "A compact four-port patch antenna for mimo application," in *2015 9th European Conference on Antennas and Propagation (EuCAP).* IEEE, 2015, pp. 1–4.

[14] C.-Y. Chiu and R. D. Murch, "Compact four-port antenna suitable for portable mimo devices," *IEEE Antennas and Wireless Propagation Letters*, vol. 7, pp. 142–144, 2008.

[15] R. S. Fakhr, A. A. Lotfi-Neyestanak, and M. Naser-Moghadasi, "Compact size and dual band semicircle shaped antenna for mimo aplications," *Progress In Electromagnetics Research C*, vol. 11, pp. 147–154, 2009.

[16] M. KOOHESTANI, "Human body proximity effects on ultra-wideband antennas," Master's thesis, Instituto Superior Tecnico, 2014.

[17] R. C. Lourenço, "Projeto de agregado conforme a uma superfície cilíndrica," Master's thesis, Instituto Superior Tecnico, 2015.

[18] J. V. Faria, "Flexible antennas design and test for human body applications scenarios," Master's thesis, Instituto Superior Tecnico, 2015.